

R. BARATE

LAPP, Chemin de Bellevue, BP110, F74941, Annecy-le-Vieux, CEDEX, France
E-mail: barate@lapp.in2p3.fr

This contribution concerns three contributed papers that share the common feature of analysing fully- (or almost fully-) reconstructed B decays coming from a sample of four million hadronic Z decays collected with the ALEPH detector at LEP. In the first paper¹, 404 charged and neutral B mesons decaying in standard modes are fully reconstructed and used to look for resonant structure in the $B\pi^\pm$ system. In the framework of Heavy Quark Symmetry (HQS), the mass of the B_2^* state and the relative production rate of the B^{**} system are measured. In the same sample of B mesons, significant $B\pi^\pm$ charge-flavour correlations are observed. In the second paper², a search for doubly-charmed B decays with both charmed mesons reconstructed is performed. A clear signal is observed in the channels $b \rightarrow D_s \bar{D}(X)$ and $b \rightarrow D \bar{D}(X)$ providing the first direct evidence for doubly-charmed b decays involving no D_s production. Evidence for associated K_S^0 and K^\pm production in the decays $B \rightarrow D \bar{D}(X)$ is also presented and some candidates for completely reconstructed B meson decays $B \rightarrow D_s \bar{D}(n\pi)$, $B \rightarrow D \bar{D} K_S^0$ and $B \rightarrow D \bar{D} K^\pm$ are observed. Furthermore, candidates for the two-body Cabibbo suppressed decays $B^0 \rightarrow D^{*+} D^{*-}$ and $B^- \rightarrow D^{*0} D^{*-}$ are also observed. One $B_s^0 \rightarrow D_s^+ D_s^-$ event is reconstructed, which can be only the short-lived CP even eigenstate. In the third paper³, the B_s decay to $D_s^{(*)+} D_s^{(*)-}(X)$ is observed, tagging the final state with two ϕ in the same hemisphere. It corresponds mostly to the short-lived CP even eigenstate. A preliminary value of the B_s short lifetime is obtained.

1 Resonant Structure and Flavour Tagging in the $B\pi^\pm$ System

1.1 Introduction

Fully reconstructed B meson decays are used to extract a precise mass of the B_2^* state and to obtain the B/\bar{B} signature at the decay point. Using the π from B^{**} decay or the nearest π from fragmentation, direct tagging of the initial B just before it oscillates and decays is possible. It could be used in future CP violation experiments.

1.2 B meson and associated pion selection

Charged and neutral B mesons are fully reconstructed in various exclusive modes. Eighty percent are in the mode^a $B \rightarrow \bar{D}^*(X)$, where X is a charged π , ρ or a_1 , and 20% are of the form $B \rightarrow J/\psi(\psi')X$, where X is a charged K or a neutral K^* . In addition, charged B candidates are reconstructed in the channels $B^- \rightarrow D^{*0}\pi^-$ and $D^{*0}a_1^-$, with a missing soft γ or π^0 from the $D^{*0} \rightarrow D^0\gamma$ or $D^0\pi^0$ decays. In total, 238 charged and 166 neutral B candidates are reconstructed with purities of $(84 \pm 3)\%$ and $(86 \pm 3)\%$ respectively.

The neighbouring pion is selected using the P_L^{max} algorithm which chooses the track with the highest projected momentum along the B direction (and a $B\pi$ mass below 7.3 GeV/c).

1.3 Resonant Structure in the $B\pi^\pm$ System

Using the pion selected with the P_L^{max} algorithm, the right sign and wrong sign $B\pi$ mass distributions are made

^aThroughout this paper, charge conjugate decay modes are always implied.

and B^{**} signals are extracted. The gain of one order of magnitude in mass resolution compared to previous inclusive experiments, due to the quality of exclusive B decays, allows a more precise measurement of the masses if one uses the Heavy Quark Symmetry parameters¹. HQS predicts 4 resonances giving 5 correlated Breit Wigner (3 narrow and 2 wide) in the $B\pi$ mass distributions. Here only the overall mass scale and the total number of signal events are left free. An unbinned likelihood fit (Fig. 1) gives :

$$M(B_2^*) = (5739_{-11}^{+8}(\text{stat})_{-4}^{+6}(\text{syst})) \text{ MeV}/c^2$$

$$f_{B^{**}} \equiv \frac{B(b \rightarrow B^{**} \rightarrow B^{(*)}\pi)}{B(b \rightarrow B_{u,d})} = (31 \pm 9(\text{stat})_{-5}^{+6}(\text{syst}))\%$$

The result for the mass of the B_2^* state is somewhat low compared to the predicted value of 5771 MeV/c².

1.4 B/\bar{B} Flavour Tagging

The sign of the neighbouring pion (from B^{**} or fragmentation) tags the B/\bar{B} nature at production : a π^+ right-sign tags a B^0 , etc. The P_L^{max} tagging algorithm efficiencies for neutral and charged B's are :

$$\epsilon_{tag}^N = (89 \pm 3(\text{stat}) \pm 2(\text{syst}))\%$$

$$\epsilon_{tag}^C = (89 \pm 2(\text{stat}) \pm 1(\text{syst}))\%$$

The asymmetry \mathcal{A}^N between the number of right-sign and wrong-sign tags, $\mathcal{A}^N = (N_{rs} - N_{ws})/(N_{rs} + N_{ws})$, is shown as a function of the B decay proper time, t , in Fig. 2a. The sinusoidal mixing of B^0 into \bar{B}^0 gives rise to the excess of wrong-sign tags (negative value of \mathcal{A}^N) at high proper times.

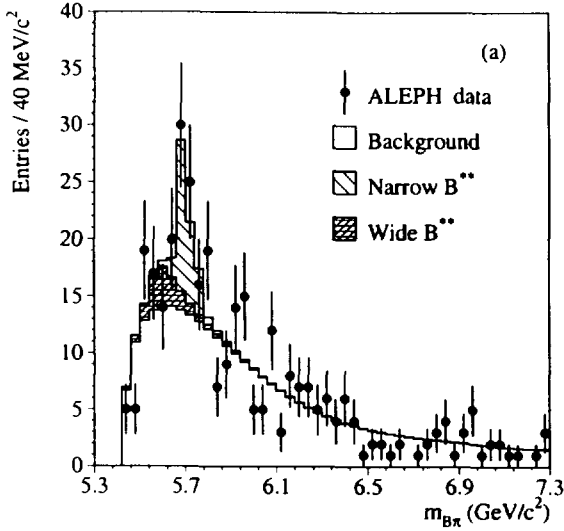


Figure 1: The $B\pi$ mass spectrum from data (points with error bars) and fit (histogram). The fit includes the expected background plus contributions from the narrow and wide B^{**} states.

The mistag rate for neutral B's, ω_{tag}^N , is measured from the oscillation amplitude, with Δm_d fixed to the world average of $0.474 \pm 0.031 \text{ ps}^{-1}$. An unbinned likelihood fit gives:

$$\omega_{tag}^N = (34.4 \pm 5.5(\text{stat}) \pm 1.0(\text{syst})) \%$$

similarly, an unbinned likelihood fit for ω_{tag}^C , the mistag rate for charged B's gives :

$$\omega_{tag}^C = (26.0 \pm 3.6(\text{stat}) \pm 0.7(\text{syst})) \%$$

showing that this method gives good tagging performance, whilst being very efficient. The corresponding fits to the data are displayed in Fig. 2.

2 Doubly charmed B decays

2.1 Introduction

The final states with 2 charm mesons allow a precise study of the b quark decay into $c\bar{c}s$ and give a direct access to the average number of charm quarks per b decay n_c . The study of 3-body B meson decay in $\bar{D}DK$ gives many results on the diagrams, possible resonances and dynamics. Added to the Cabibbo suppressed $\bar{D}\bar{D}$, standard $D_s^+\bar{D}$, and new $D_s^+\bar{D}n\pi^\pm$ decays, one obtains the total double charm contribution to B meson decay.

2.2 $\bar{D}\bar{D}$ selection

The charmed mesons are searched for in the decay modes $D^0 \rightarrow K^-\pi^+$, $D^0 \rightarrow K^-\pi^+\pi^-\pi^+$,

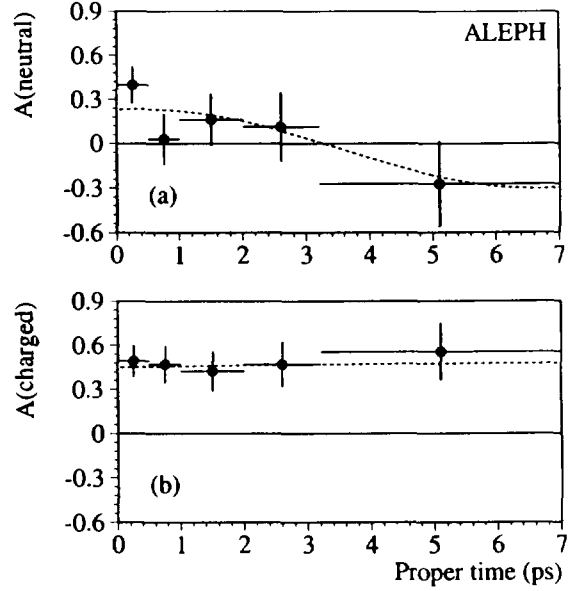


Figure 2: The right-sign/wrong-sign asymmetries in the data as a function of the proper decay time. The dashed curves display the charge asymmetries determined from the unbinned likelihood fits.

$D^+ \rightarrow K^-\pi^+\pi^+$, $D^{*+} \rightarrow D^0\pi^+$, $D_s^+ \rightarrow \phi\pi^+$ ($\phi \rightarrow K^-K^+$) and $D_s^+ \rightarrow \bar{K}^{*0}K^+$ ($\bar{K}^{*0} \rightarrow K^-\pi^+$). For D^0 mesons from D^{*+} decay, the decay mode $D^0 \rightarrow K^-\pi^+\pi^0$ is also used.

The pairs of D candidates must be in the same hemisphere and the two D candidates are required to form a vertex with a probability of at least 0.1%. To maintain a good acceptance for the $B \rightarrow \bar{D}\bar{D}X$ signal whilst rejecting the backgrounds and minimizing the model dependence of the selection efficiencies, a cut $d_{BD}/\sigma_{BD} > -2$ (>0) is applied on the D^0 , D_s^+ (D^+) decay length significance (defined in Fig. 3). The decay length significance of the $\bar{D}\bar{D}$ vertex is also required to satisfy the condition $d_B/\sigma_B > -2$.

To obtain the number of real $\bar{D}\bar{D}$ events, standard tables are made (for instance $m(K\pi)_1/m(K\pi)_2$) and the combinatorial background is subtracted linearly.

2.3 Inclusive b quark decays in $D_s\bar{D}(X)$ or $\bar{D}\bar{D}(X)$

After acceptance corrections, the different branching fractions obtained are given in Table 1.

The inclusive branching fraction of b quarks to $D_s\bar{D}(X)$ is measured to be

$$\mathcal{B}(b \rightarrow D_s D^0, D_s D^\pm(X)) = (13.1_{-2.2}^{+2.6}(\text{st})_{-1.6}^{+1.8}(\text{sy})_{-2.7}^{+4.4}(\mathcal{B}_D))\%$$

in good agreement with previous measurements of the inclusive branching fraction of the B mesons to D_s .

For the first time, doubly-charmed B decays involving no D_s production are observed. The corresponding

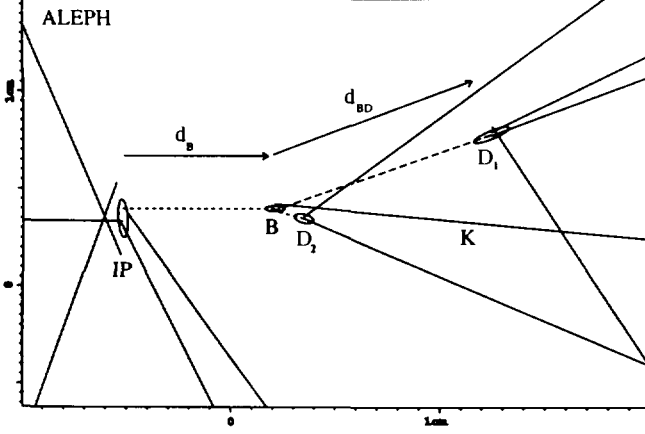


Figure 3: Display of a decay $B^0 \rightarrow D^- D^0 K^+$ reconstructed in the ALEPH detector (real data).

Table 1: Summary of the different branching fractions measured in this analysis. The modes involving a D^{*+} (lowest part of the table) are also included in the upper part results as a subsample of the modes involving a D^0 or a D^+ .

Channel	$\mathcal{B}(\%)$
$b \rightarrow D^0 D_s^-(X)$	$9.1^{+2.0}_{-1.8} {}^{+1.3}_{-1.2} {}^{+3.1}_{-1.9}$
$b \rightarrow D^+ D_s^-(X)$	$4.0^{+1.7}_{-1.4} \pm 0.7 {}^{+1.4}_{-0.9}$
Sum $b \rightarrow D^0 D_s^-, D^+ D_s^-(X)$	$13.1^{+2.6}_{-2.2} {}^{+1.8}_{-1.6} {}^{+4.4}_{-2.7}$
$b \rightarrow D^0 \bar{D}^0(X)$	$5.1^{+1.6}_{-1.4} {}^{+1.2}_{-1.1} \pm 0.3$
$b \rightarrow D^0 D^-, D^+ \bar{D}^0(X)$	$2.7^{+1.5}_{-1.3} {}^{+1.0}_{-0.9} \pm 0.2$
$b \rightarrow D^+ D^-(X)$	$< 0.9\% \text{ at } 90\% \text{ C.L.}$
Sum $b \rightarrow D^0 \bar{D}^0, D^0 D^-, D^+ \bar{D}^0(X)$	$7.8^{+2.0}_{-1.8} {}^{+1.7}_{-1.5} {}^{+0.5}_{-0.4}$
$b \rightarrow D^{*+} D_s^-(X)$	$3.3^{+1.0}_{-0.9} \pm 0.6 {}^{+1.1}_{-0.7}$
$b \rightarrow D^{*+} \bar{D}^0, D^0 D^{*-}(X)$	$3.0^{+0.9}_{-0.8} {}^{+0.7}_{-0.5} \pm 0.2$
$b \rightarrow D^{*+} D^-, D^+ D^{*-}(X)$	$2.5^{+1.0}_{-0.9} {}^{+0.6}_{-0.5} \pm 0.2$
$b \rightarrow D^{*+} D^{*-}(X)$	$1.2^{+0.4}_{-0.3} \pm 0.2 \pm 0.1$

inclusive branching fractions are

$$\mathcal{B}(b \rightarrow D^0 \bar{D}^0, D^0 D^\pm(X)) = (7.8^{+2.0}_{-1.8}(\text{st}) {}^{+1.7}_{-1.5}(\text{sy}) {}^{+0.5}_{-0.4}(\mathcal{B}_D))\%$$

Hence a significant fraction of the doubly-charmed B decays leads to no D_s production. For the average mixture of b hadrons produced at LEP, the sum over all the decay modes above yields:

$$\mathcal{B}(b \rightarrow D_s D^0, D_s D^\pm, D^0 \bar{D}^0, D^0 D^\pm(X)) = (20.9^{+3.2}_{-2.8}(\text{stat}) {}^{+2.5}_{-2.2}(\text{syst}) {}^{+4.5}_{-2.8}(\mathcal{B}_D))\%.$$

Adding the small hidden charm and charmed baryon contributions, this measurement is in good agreement with the recent ALEPH measurement of the average number of charm quarks per b decay :

$$n_c = 1.230 \pm 0.036(\text{stat}) \pm 0.038(\text{syst}) \pm 0.053(\mathcal{B}_D).$$

Some corresponding $D^{(*)} \bar{D}^{(*)}$ mass spectra are given in Fig. 4.

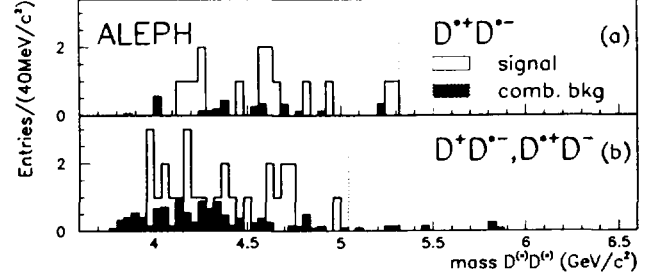


Figure 4: Unshaded histogram: the $D\bar{D}$ mass spectra of the selected $b \rightarrow D\bar{D}(X)$ candidates (a) $D^{*+} D^{*-}$ (b) $D^\pm D^{*\mp}$. The channels are mutually exclusive. Shaded histogram: the $D\bar{D}$ mass distribution of the events in the sidebands of the D_1 or D_2 mass spectra, normalised to the expected number of combinatorial background events.

2.4 Cabibbo suppressed $B \rightarrow \bar{D}D$ decays

As can be seen in Fig. 4a, two candidates for the Cabibbo suppressed decay $B_d^0 \rightarrow D^{*+} D^{*-}$ are observed. Asking for no charged track at the $D\bar{D}$ vertex, the background is reduced to 0.10 ± 0.03 event. The corresponding branching fraction is measured to be

$$\mathcal{B}(\bar{B}_d^0 \rightarrow D^{*+} D^{*-}) = (0.23^{+0.19}_{-0.12} \pm 0.04 \pm 0.02(\mathcal{B}_D))\%.$$

One candidate for the Cabibbo suppressed decay $B^- \rightarrow D^{*-} D^0$, with both D vertices well separated from the reconstructed B decay point, is also observed⁴ and limits on branching fractions are obtained².

2.5 Semi inclusive $B \rightarrow \bar{D}DK(X)$ decays

Reconstructing a K_S^0 and K^\pm compatible with the $D\bar{D}$ vertex, and making the $\bar{D}DK$ invariant mass (without using the soft pion from a D^*), 3 peaks separated by about 150 MeV/c^2 appear, corresponding to the three 3-body B meson decay modes (Fig. 5). At a lower mass, the events correspond to more than 3-body decay modes (mainly $D^{(*)} \bar{D}^{(*)} K\pi$). After background subtraction, the total number of events is 32.2 ± 7.9 , and in the 3-body region 21.2 ± 5.5 . Hence, one sees that the three-body decays $B \rightarrow \bar{D}^{(*)} D^{(*)} K$ are a large part (about 70%) of the inclusive doubly-charmed $B \rightarrow \bar{D}^{(*)} D^{(*)} K(X)$ decays.

2.6 Exclusive $B \rightarrow \bar{D}DK$ decays

Asking now for no other charged track at the $\bar{D}DK$ vertex (and using the soft pion from a D^* when available), a clear B signal appear (Fig. 6) with 9 $\bar{D}^{(*)} D^{(*)} K_S^0$ events and 9 $\bar{D}^{(*)} D^{(*)} K^\pm$ events above 5.04 GeV/c^2 . One of these events⁴ was displayed in Fig. 3.

No evidence for resonant decays $B \rightarrow \bar{D}^{(*)} D_{s1}^+$ (2535) is found.

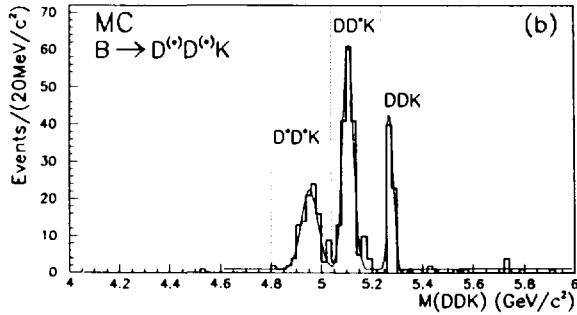
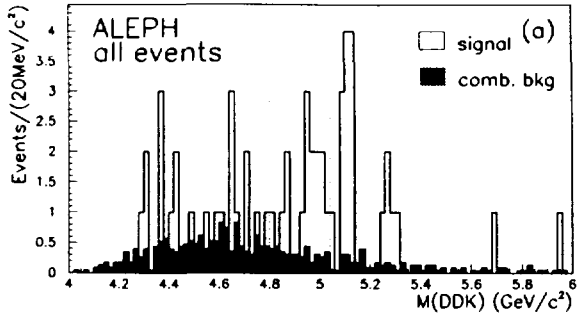


Figure 5: The $D^0\bar{D}^0K$, D^0D^-K or D^+D^-K mass of $D\bar{D}$ events with a reconstructed K_S^0 or a K^\pm for (a) ALEPH data (b) simulated three-body decays $B \rightarrow D^{(*)}\bar{D}^{(*)}K$. The π^+ from $D^{*+} \rightarrow D^0\pi^+$, even if reconstructed, are not used in the mass.

B and \bar{B} decays give different final states and, for instance in a \bar{B} decay, the D coming from the b quark decay (called D_b) can be distinguished from the \bar{D} coming from the W decay (D_W): in most of the events, the invariant mass $m(D_bK)$ tend to be higher than $m(D_WK)$ (and hence the momentum $p(D_b)$ in the B rest frame is higher than $p(D_W)$).

The diagrams contributing to these decays can be divided into 3 classes (Table 2): External W (E), Internal W (I) or color suppressed (cf $B \rightarrow J/\psi K$) and interference (EI); as can be seen in Table 2, some I type events are also observed.

Using isospin symmetry, the different branching fractions are given in Table 2 and the sum is :

$$\mathcal{B}(B \rightarrow \bar{D}^{(*)}D^{(*)}K) = (7.1_{-1.5}^{+2.5}(\text{st})_{-0.8}^{+0.9}(\text{sy}) \pm 0.5(\mathcal{B}_D))\%.$$

2.7 $B \rightarrow \bar{D}DKX$ decays

Compared to the semi-inclusive result of Sec. 2.5 or to the inclusive b results of Sec. 2.3, scaled by a factor $1/2f_{D^0} = 1.3$ to account for $b \rightarrow \bar{B}^0, B^-$, one sees that $\mathcal{B}(B \rightarrow \bar{D}^{(*)}D^{(*)}KX)$ should be about 3%.

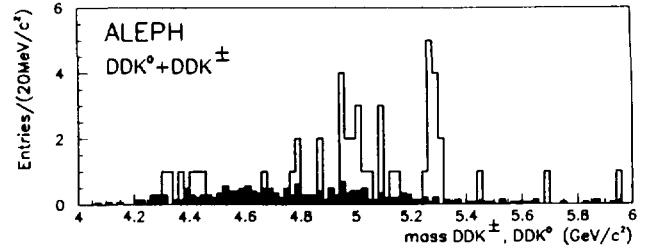


Figure 6: Invariant mass $m(D\bar{D}K)$ for events with one identified K and no other additional track from the $D\bar{D}K$ vertex. D can be either a D^0 , a D^+ or a D^{*+} .

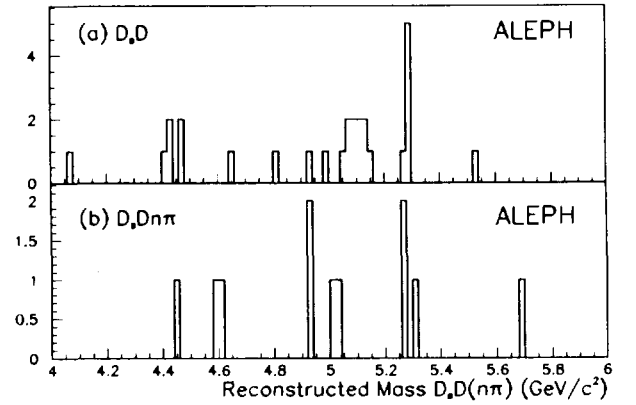


Figure 7: Invariant mass $m(D_s^+ \bar{D}(n\pi^\pm))$ reconstructed for ALEPH data (a) $D_s^+ \bar{D}$ (b) $D_s^+ \bar{D}n\pi^\pm$, $n \geq 1$. The peak close to $5.1 \text{ GeV}/c^2$ is due to events with one missing neutral from decays $D^{*+} \rightarrow D^0\pi^+$, γ or or $D_s^{*+} \rightarrow D_s^+\gamma$.

2.8 $B \rightarrow D_s^+ \bar{D}(n\pi^\pm)$ decays

Using the events with a $D_s^+ \bar{D}$ mass above $5.04 \text{ GeV}/c^2$ in Fig. 7a, the branching fraction of B^0 and B^+ mesons into doubly-charmed two-body decay modes is also measured and gives

$$\mathcal{B}(B \rightarrow D_s^{(*)+} \bar{D}^{(*)}) = (5.6_{-1.5}^{+2.1}(\text{st})_{-0.8}^{+0.9}(\text{sy})_{-1.1}^{+1.9}(\mathcal{B}_D))\%,$$

in good agreement with previous measurements of the same quantity.

For the first time, some candidates for completely reconstructed decays $B^0, B^+ \rightarrow \bar{D}^{(*)}D_s^+ n\pi^\pm$ ($n \geq 1$) are also observed (Fig. 7b). A measurement of the branching fraction for many-body decays $B^0, B^+ \rightarrow \bar{D}^{(*)}D_s^+ X$ is performed, leading to

$$\mathcal{B}(B \rightarrow D_s^{(*)\pm} D^{(*)} X) = (9.4_{-3.1}^{+4.0}(\text{st})_{-1.8}^{+2.2}(\text{sy})_{-1.6}^{+2.6}(\mathcal{B}_D))\%.$$

Table 2: Summary of the various branching fractions $B \rightarrow D\bar{D}K$ measured in this analysis.

Diagram	Channel (B^0, B^+)	Number of candidates	$\mathcal{B}(B \rightarrow D^{(*)}\bar{D}^{(*)}K)$ (B^0/B^+ average)
E	$D^-D^0K^+, \bar{D}^0D^+K^0$	3	$1.7^{+1.2}_{-0.8} \pm 0.2 \pm 0.1\%$
E	$(D^{*-}D^0 + D^-D^{*0})K^+, (\bar{D}^{*0}D^+ + \bar{D}^0D^{*+})K^0$	5	$1.8^{+1.0}_{-0.8} \pm 0.3 \pm 0.1\%$
E	$D^{*-}D^{*0}K^+, \bar{D}^{*0}D^{*+}K^0$	1	$< 1.3\%$
I	$\bar{D}^0D^{*0}K^0, D^+D^-K^+$	1	$< 2.0\%$
I	$(\bar{D}^0D^{*0} + \bar{D}^{*0}D^0)K^0, (D^{*+}D^- + D^+D^{*-})K^+$	1	$< 1.6\%$
I	$\bar{D}^{*0}D^{*0}K^0, D^{*+}D^{*-}K^+$	1	$< 1.5\%$
EI	$D^+D^-K^0, \bar{D}^0D^0K^+$	1	$< 1.9\%$
EI	$(D^{*+}D^- + D^+D^{*-})K^0, (\bar{D}^{*0}D^0 + \bar{D}^0D^{*0})K^+$	4	$1.6^{+1.0}_{-0.7} \pm 0.2 \pm 0.1\%$
EI	$D^{*+}D^{*-}K^0, \bar{D}^{*0}D^{*0}K^+$	1	$< 3.0\%$
Sum E	$D^{(*)-}D^{(*)0}K^+, \bar{D}^{(*)0}\bar{D}^{(*)+}K^0$	9	$3.5^{+1.7}_{-1.1} \pm 0.5 \pm 0.2\%$
Sum I	$\bar{D}^{(*)0}D^{(*)0}K^0, D^{(*)+}D^{(*)-}K^+$	3	$0.8^{+1.0}_{-0.4} \pm 0.2 \pm 0.1\%$
Sum EI	$D^{(*)+}D^{(*)-}K^0, \bar{D}^{(*)0}D^{(*)0}K^+$	6	$2.8^{+1.6}_{-1.0} \pm 0.4 \pm 0.2\%$
E+I+EI	Sum DDK	5	$2.3^{+1.5}_{-0.9} \pm 0.3 \pm 0.2\%$
E+I+EI	Sum $D\bar{D}^*K + D^*\bar{D}K$	10	$3.8^{+1.6}_{-1.1} \pm 0.5 \pm 0.2\%$
E+I+EI	Sum $D^*\bar{D}^*K$	3	$1.0^{+1.3}_{-0.6} \pm 0.2 \pm 0.1\%$
E+I+EI	Sum $D^{(*)}\bar{D}^{(*)}K$	18	$7.1^{+2.5}_{-1.5} \pm 0.9 \pm 0.5\%$

2.9 Conclusion on B meson decays

Summing the results of Sec. 2.4, 2.6, 2.7 and 2.8, one sees that $B \rightarrow D\bar{D}(X)$ and $B \rightarrow D_s^+\bar{D}(X)$ are a big part (about 25%) of B mesons decays.

2.10 $B_s^0 \rightarrow D_s^+D_s^-$ decay

One event⁴ is reconstructed with a $D_s^+D_s^-$ mass at the B_s^0 mass, on a negligible background, with $D_s^+ \rightarrow \bar{K}^{*0}K^+$ and $D_s^- \rightarrow \phi\pi^-$. This can be only the pure CP even B_s^0 short state as explained in Sec. 3.1 below.

3 Width difference in the $B_s - \bar{B}_s$ system

3.1 Introduction

Most of the channels common to B_s and \bar{B}_s are CP even (cf $D_s^+D_s^- \dots$). Hence the B_s short is the CP even state. Here a direct measurement of the B_s short lifetime is made using the mostly CP even decay modes $B_s^0 \rightarrow D_s^{(*)+}D_s^{(*)-}(X)$ with $D_s^+ \rightarrow \phi X$, that is a $\phi\phi X$ final state⁵.

3.2 $\phi\phi$ selection

The same method as for double charm (Sec. 2.2) is applied (table $m(K^+K^-)_1/m(K^+K^-)_2$). The number of $\phi\phi$ events measured in this way is $N_{\phi\phi} = 50 \pm 15$, taking into account the non linear background shape near the K^+K^- threshold. In these events, 20% of charm contamination is expected from Monte Carlo;

the contribution of $\phi\phi$ coming from B_d and B_u decays is evaluated using $\mathcal{B}(B \rightarrow D_s^{(*)\pm}D^{(*)}(X))$ measured in Sec. 2.8. After subtracting these events, the number of $B_s^0 \rightarrow D_s^{(*)+}D_s^{(*)-}(X)$ found is $N_{sig} = 32 \pm 17$ (over a background of 78%). This number corresponds to a $B_s^0 \rightarrow D_s^{(*)+}D_s^{(*)-}(X)$ branching ratio of approximately 10%.

3.3 B_s short lifetime

The $\phi\phi$ vertex (which has a resolution of about $200\mu m$) is a good approximation of the B_s vertex due to the short D_s lifetime. An unbinned maximum likelihood fit using background parametrisation from the sidebands gives a preliminary lifetime $\tau_s = 1.42 \pm 0.23 \pm 0.16$ ps for this eigenstate. Using the world average B_s lifetime, $\bar{\tau} = 1.61 \pm 0.10$ ps, it would correspond⁵ to $\Delta\Gamma/\Gamma = (24 \pm 35)\%$ where the statistical and systematic errors are combined.

References

1. Paper # 946, Preprint CERN EP/98-017, submitted to *Phys. Lett. B*.
2. Paper # 941, Preprint CERN EP/98-037, submitted to *The European Physical Journal C*.
3. Paper # 1054, Preprint ALEPH 98-064.
4. Color displays of the events shown during the talk can be found in <http://alephwww.cern.ch/>.
5. See also A. Ribon, Talk # 802, these proceedings.